Wideband Measurements of Channel Characteristics at 2.4 and 5.8 GHz in Underground Mining Environments

Ahmed BENZAKOUR [1,3], Sofiène AFFÈS [1,3], Charles DESPINS [1,2,3] *and* Pierre-Martin TARDIF [1,3]

1: INRS-Énergie Matériaux et Télécommunications, Montreal, Canada 2: PROMPT-Québec, Montreal, Canada
3: Underground Communications Research Laboratory (LRCS), Val d'Or, Canada

Abstract- This paper analyzes the results of wideband radio channel measurements conducted in an underground mining environment at center frequencies of 2.4 GHz and 5.8 GHz using a vector network analyzer. Relevant impulse response parameters such as the rms delay spread and the relative multipath total power are presented and compared for the two bands. The measurements suggest that in such an underground gallery and in the two frequency bands, random reflections have the effect of flattening the relationship between the rms delay spread and distance. In the 2.4 GHz band, the rms delay spread is less than or equal to 6.34 nanoseconds for 90% of all measurement locations. The corresponding value for the 5.8 GHz band is 4.98 nanoseconds. In general, it has been observed that underground radio channel characteristics are influenced by the configuration of this peculiar environment.

Index terms – Wideband measurement, Underground mine, RMS delay spread, Relative multipath total power.

I. INTRODUCTION

Measuring and characterizing the impulse response parameters of mobile radio channels is important in the design process and implementation of efficient and reliable mobile systems. In particular, a good communication system in underground mines can largely increase safety and production output. To date, however, there are few studies available in the literature which consider this peculiar environment [1-6].

This paper details the results of wideband propagation measurements at center frequencies of 2.4 GHz and 5.8 GHz, made in the CANMET (Canadian Center for Minerals and Energy Technology) experimental mine in Val d'Or (Québec). The two frequencies are compared by evaluating the rms delay spread and the relative multipath power.

In our study, radio channel sounding was carried out in the frequency domain. This technique is based on sweeping the measured bandwidth with a single sine wave signal. In a post-processing step, the recorded radio channel frequency responses are inverse-Fourier transformed to get the channel impulse responses. Finally, the channel characterization is obtained from the impulse responses.

This paper is organized as follows. Section II provides a description of the underground environment and of the channel measurement system. In section III the analysis of the collected data is performed. Section IV draws out the conclusions of this work.

II. DESCRIPTION OF THE ENVIRONMENT AND THE CHANNEL MEASUREMENT SYSTEM

Experiments were conducted in an underground gallery of a former gold mine, the laboratory mine CANMET in Val d'Or, 500 kilometers north west of Monteal, Canada. Located at a 70 m underground level, the gallery stretches over a length of 70 meters with 2.5 to 3 meters of width and approximately 3 meters of height. A plan of the gallery is provided in *Figure 1*.

Due to the curvature of the gallery, the existence of non-line-of-sight (NLOS) cases is visible. Moreover, the walls are very rough, the floor is not flat and it contains some large puddles of water.

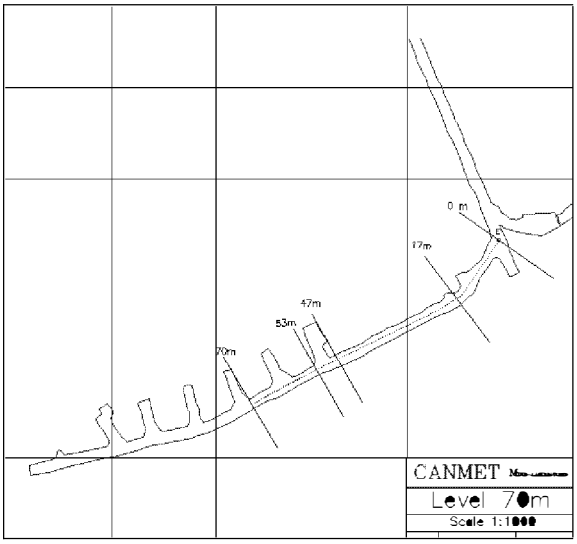

Figure 1. *Map of the underground gallery.*

To investigate the statistical behavior of the channel, experiments were conducted in which channel impulse response structures in the two bands of interest were compared for 420 different receiver locations along the gallery, while the transmitter remained fixed. For each location, a temporal average has been performed on a

set of ten complex-transform-function measurements at different observation times.

The wideband measurement setup consisted of a vector network analyzer with fixed and moving onmidirectional antennas to act as the receiver and transmitter, respectively. The transmitting port swept the channel in the 2.3-2.5 GHz frequency band (5.7-5.9 GHz resp.) and the receiving port recorded the channel output with the signal attenuation and phase shift introduced by the channel in the frequency domain. The received data was then transformed to the time domain using the Fourier transform to obtain the time delay profile. The frequency step covering the 2.3-2.5 GHz frequency band (5.7-5.9 GHz resp.) was set to 200 MHz. Consequently in the time domain a theoretical resolution of 5 ns was obtained (in practice, due to the use of windowing, the time resolution is estimated to be around 8 ns).

During the measurements, transmit and receive antennas were both at a height of 1.8 meters.

III. EXPERIMENTAL RESULTS

A. Typical frequency and time domain responses

The magnitude in dB of a typical frequency response as measured by the vector network analyzer is presented in *Figure 2*. Notches in the magnitude curve illustrate the frequency selective nature of fading in the indoor galery channel. The phase is mostly linear except for large phase shifts which occur when deep fades are present.

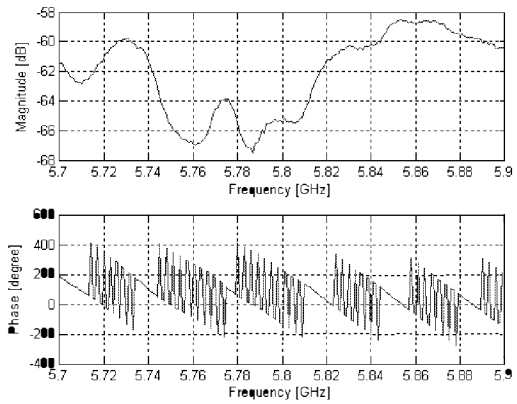

Figure 2. *Magnitude and phase of a typical measured frequency response.*

The magnitude of the computed time domain response corresponding to the frequency response measurement of *Figure 2* is given in *Figure 3*. Multipath components with various delays can be clearly seen.

(a)

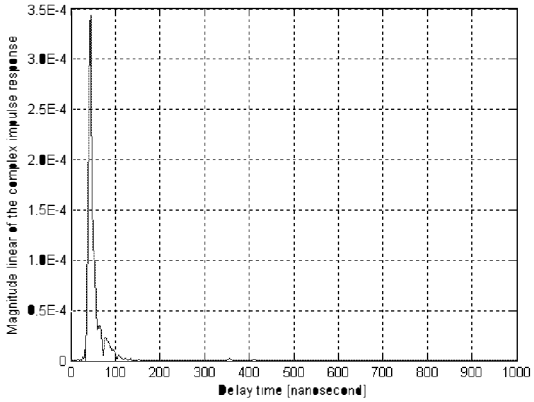

(b)

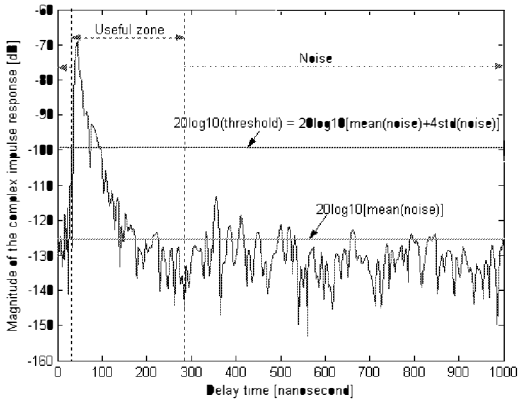

Figure 3. *Magnitude of the computed time domain response for a specific TX-RX separation: (a) linear and (b) dB unit.*

B. Relevant impulse response parameters

The time dispersion parameters, the relative multipath total power P and the number of multipath components N were computed. Their statistics were then extracted from the magnitude of the complex impulse response of the channel in the two bands of interest, at all 420 measurement locations by using predefined thresholds for the multipath noise floor.

The time dispersion parameters are [8]:

- ***Mean excess delay*** is the first moment of the power delay profile defined by:

$$\tau_m = \frac{\sum_k P(\tau_k).\tau_k}{\sum_k P(\tau_k)} .$$

- ***RMS delay spread*** is the square root of the second central moment of the power delay profile given by:

$$\tau_{rms} = \sqrt{\frac{\sum_k [\tau_k - \tau_m]^2 . P(\tau_k)}{\sum_k P(\tau_k)}} .$$

- ***Maximum excess delay*** is the time delay during which multipath energy falls to X dB below the maximum.

Here we have used a relative signal threshold. The value of the threshold, however, has a dramatic effect on the resultant parameters one extracts from the measurements. Our statistical analysis is based on a noise threshold set to four times the standard deviation plus the mean of the noise measured over the tail of the impulse response (see *Figure 3*).

Figures 4(a) and *4(b)* plot τ_{rms} against the transmit-receive antenna separation at 2.4 GHz and 5.8 GHz, respectively.

(a)

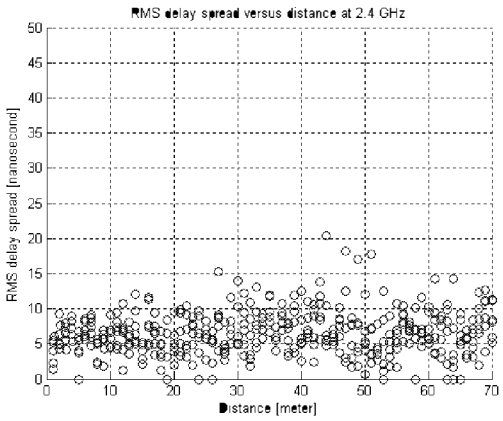

(b)

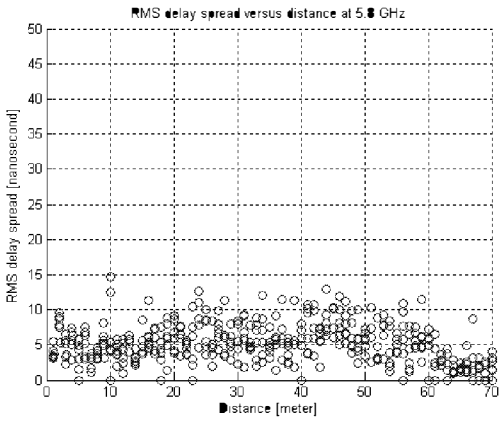

Figure 4. *RMS delay spread as a function of distance at (a): 2.4 GHz and (b): 5.8 GHz*

For the underground gallery considered and in the two frequency bands, random reflections have the effect of flattening the relationship between the rms delay spread and distance. In contrast, we have not seen the same phenomenon at the 40 m level of the mine [5], where the gallery is 5 meters large. In both cases, the profiles observed differ from those commonly found in indoor building environments [6] [7].

Results thus show that indoor underground multipath characteristics can vary considerably depending upon the gallery dimensions and the transmit/receive distance.

In *Figure 5*, the cumulative distribution function (CDF) of τ_{rms} for both bands shows the percentage of receive locations for which the rms delay spread is less than a specified value.

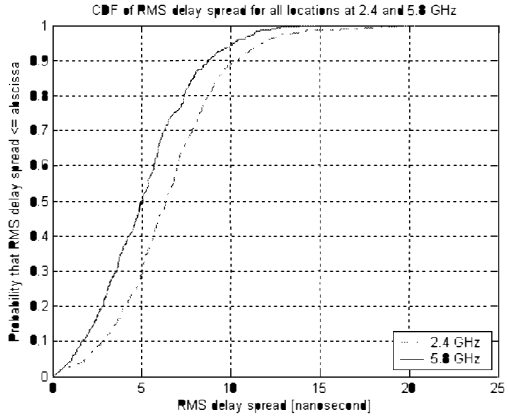

Figure 5. *Cumulative distribution function of τ_{rms} at 2.4 and 5.8 GHz.*

As the delay spreads were greater at 2.4 GHz in several locations (*Figures 4 (a)* and *(b)*), the CDF plot for that band is consequently below that for the 5.8 GHz. It can be seen that in the 2.4 GHz band, the rms is less than or equal to 6.34 nanoseconds for 50 % of all locations. The corresponding value for the 5.8 GHz band is 4.98 nanoseconds.

For the wideband radio systems in such environment, performance levels under static conditions would be marginally better in the 5.8 GHz band, since delay spreads are slightly smaller in this band than at 2.4 GHz. But coverage would be about the same for both bands.

The mean, the standard deviation and the maximum of τ_m , τ_{rms} and τ_{max} at both bands have been computed from the time domain responses and summarized in *Table 1*.

Table 1. *Mean, standard deviation and maximum of τ_m, τ_{rms} and τ_{max} at 2.4 GHz and 5.8 GHz.*

All locations	*mean*		*std*		*max*	
	2.4 GHz	*5.8 GHz*	*2.4 GHz*	*5.8 GHz*	*2.4 GHz*	*5.8 GHz*
τ_m (nsec)	3.21	2.30	3.24	2.61	18.51	15.83
τ_{rms} (nsec)	6.49	5.11	3.07	2.74	20.40	14.74
τ_{max} (nsec)	42.38	46.23	30.76	45.62	232	240

Plots against distance of the relative multipath total power *P* and the number of multipath components *N*, at both bands, are shown in *Figures 6* and *7*, respectively.

Figures 6(a) and *6(b)* show that the curvature of the gallery located at about 17 meters from the transmitter does not have a visible effect on the attenuation of the signal in both frequency bands. That may be explained by the narrow dimensions of the gallery and the position of the transmitter close to the curvature. However, an abrupt fall in the power of the signal in the 2.4 GHz band was noticed for the two transmitter-receiver spacings of 43 and 44 meters. The same phenomenon was noticed around 70 meters at 2.4 GHz. That can be explained by the multipath destructive combinations. On the other hand, a slight increase in the multipath total power for some receiver locations, at both frequency bands, was recorded between 47 and 53 meters. Since the number of multipath components vary marginally at these distances (*Figures 7(a)* and *7(b)*), this increase is probably a result of the variation in the phase of the paths induced by the first connecting gallery (this gallery is about 7 meters deep), possibly implying constructive combinations. This is more visible in the 2.4 GHz band.

(a)

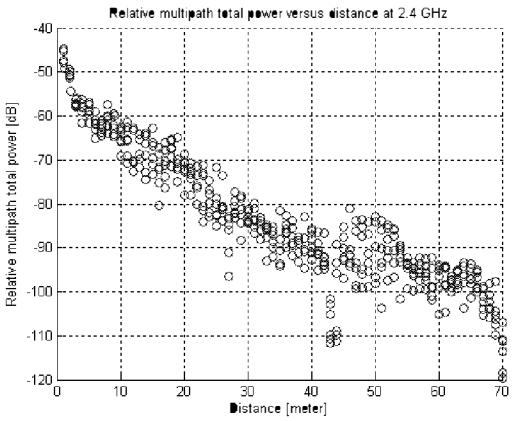

(b)

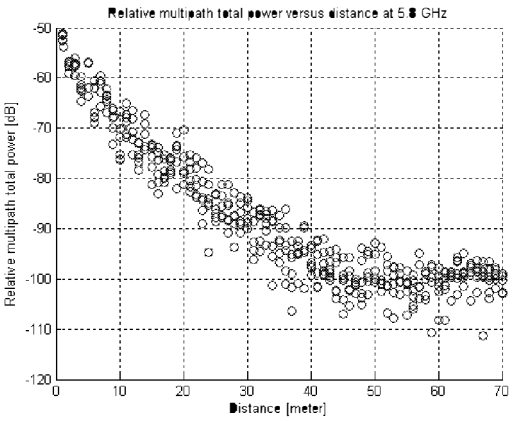

Figure 6. *Relative multipath total power as a function of distance at (a): 2.4 GHz and (b): 5.8 GHz.*

(a)

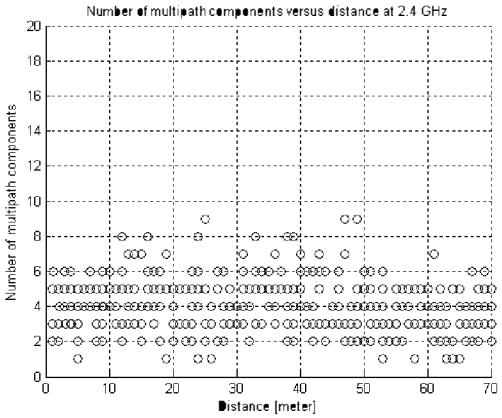

(b)

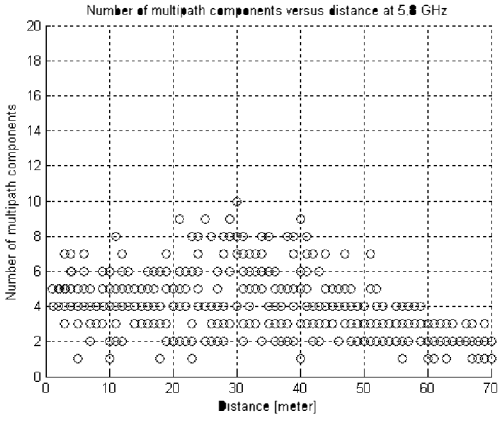

Figure 7. *Number of multipath components as a function of distance at (a): 2.4 GHz and (b): 5.8 GHz.*

The mean value, the standard deviation and the maximum value of *N* for all locations at 2.4 GHz and 5.8 GHz are given in ***Table 2***.

Table 2. *Mean, standard deviation and maximum of N at 2.4 GHz and 5.8 GHz.*

All locations	*mean*		*std*		*max*	
	2.4 GHz	*5.8 GHz*	*2.4 GHz*	*5.8 GHz*	*2.4 GHz*	*5.8 GHz*
N	4	3.9	1.5	1.8	9	10

IV. SUMMARY AND CONCLUSIONS

In order to characterize radio channels in underground mines, measurements were performed at 2.4 and 5,8 GHz using a vector network analyzer. Frequency responses were obtained for one transmitter location and 420 receiver locations in an underground gallery. The inverse Fourier transform was used to convert the frequency domain data to corresponding time domain responses.

Results show that indoor underground multipath characteristics can vary considerably depending upon the gallery dimensions and the transmit/receive antenna separation. They also suggest that random reflections have the effect of flattening the relationship between the rms delay spread and distance in the gallery considered at both frequency bands of 2.4 and 5.8 GHz.

For the studied environment, performance levels under static conditions would be marginally better in the 5.8 GHz band, but coverage would be about the same for both bands.

The results presented herein are currently exploited in the design of wireless local area networks and for radiolocation applications [9] in an underground mining environment.

ACKNOWLEDGMENT

The authors wish to thank Mathieu BOUTIN, Mourad DJADEL and Chahé NERGUIZIAN for their precious cooperation.

REFERENCES

[1] M. Linéard and P. Degauque, "Natural Wave Propagation in Mine Environments", IEEE Trans. on Antennas and Propagation, Vol. 48, No.9, pp. 1326 - 1339, September 2000.

[2] Y.P. Zhang, G.X. Zheng and J.H. Sheng, "Radio Propagation at 900 MHz in Underground Coal Mines", IEEE Trans. On Antenna and Propagation, Vol. 49, No.5, pp. 757 - 762, May 2001.

[3] M. Djadel, C. Despins and S. Affès, "Narrowband Propagation Characteristics at 2.45 and 18 GHz in Underground Mining Environments", Proc. IEEE GLOBCOM, 2002, pp. 1870 - 1874.

[4] B.L.F. Daku, W. Hawkins and A.F. Prugger, "Channel Measurements in Mine Tunnels", Proc. IEEE VTC Spring, 2002, Vol. 1, pp. 380 - 383.

[5] C. Nerguzian, M. Djadel, C. Despins and S. Affes, "Narrowband and Wideband Radio Channel Characteristics in Underground Mining Environments at 2.4 GHz", Proc. IEEE PIMRC, 2003, Vol.1, pp. 680 - 684.

[6] R.J.C. Bultitude at al., "The Dependence of Indoor Radio Channel Multipath Characteristics on Transmit/Receive Ranges", IEEE JSAC, Vol.11, No.7, pp. 979 - 990, September 1993.

[7] A.F. AbouRaddy, S.M. Elnoubi and A. El-Shafei, "Wideband Measurements and Modeling of the Indoor Radio Channel at 10 GHz", Parts I and II, Proc. 15th National Radio Science Conference, 1998, pp. B13/1 - B13/8 and B14/1 - B14/8.

[8] T.S. Rappaport, "Wireless Communications: Principles and Practice", Prentice Hall, Second Edition, 2002

[9] C. Nerguzian, C. Despins and S. Affes, "Geolocation in Mines with an Impulse Response Fingerprinting Technique and Neural Networks", Proc. IEEE VTC Fall, 2004, to appear.